Inhibition of Recombinant Cytochrome P450 Isoforms 2D6 and 2C9 by Diverse Drug-like Molecules

Daniel R. McMasters,*,† Rhonda A. Torres,†,‡ Susan J. Crathern,§ Deborah L. Dooney,§ Robert B. Nachbar,∥ Robert P. Sheridan,† and Kenneth R. Korzekwa§

Department of Molecular Systems and Department of Applied Computer Science and Mathematics, Merck Research Laboratories, Rahway, New Jersey, and Department of Drug Metabolism, Merck Research Laboratories, West Point, Pennsylvania

Received January 3, 2007

The affinities of a diverse set of 500 drug-like molecules to cytochrome P450 isoforms 2C9 and 2D6 were measured using recombinant expressed enzyme. The dose−response curve of each compound was fitted with a series of equations representing typical or various types of atypical kinetics. Atypical kinetics was identified where the Akaike Information Criterion, plus other criteria, suggested the kinetics was more complex than expected for a Michaelis−Menten model. Approximately 20% of the compounds were excluded due to poor solubility, and approximately 15% were excluded due to fluorescence interference. Of the remaining compounds, roughly half were observed to bind with an affinity of 200 μM or lower for each of the two isoforms. Atypical kinetics was observed in 18% of the compounds that bind to cytochrome 2C9, but less than 2% for 2D6. The resulting collection of competitive inhibitors and inactive compounds were analyzed for trends in binding affinity. For CYP2D6, a clear relationship between polar surface area and charge was observed, with the most potent inhibitors having a formal positive charge and a low percent polar surface area. For CYP2C9, no clear trend between activity and physicochemical properties could be seen for the group as a whole; however, certain classes of compounds have altered frequencies of activity and atypical kinetics.

Introduction

The cytochrome P450 enzymes (CYPs) are versatile enzymes that can oxidize a wide variety of hydrophobic compounds. The ability to metabolize a diverse set of substrates is required for the eventual removal of foreign compounds. This versatility is accomplished because the enzymes generate highly reactive species of oxygen,[1,2] have relatively nonspecific substrate binding interactions, and because there is a superfamily of CYPs with overlapping substrate selectivities. Three CYPs 3A4, 2D6, and 2C9 are responsible for the microsomal oxidation of a majority of drugs in the human. Because relatively few enzymes are responsible for the metabolism of many different drugs, administration of one drug can result in the inhibition of the metabolism of other co-administered drugs. As a result, inhibition of CYPs by a drug is an important cause of drug−drug interactions (DDI[a]). To avoid dangerous interactions as well as prevent the need for specially designed clinical trials to assess DDI potential, it is advantageous to select clinical candidates that are not high-affinity inhibitors of the major CYPs. For this reason, in vitro screens have been extensively used to measure the affinity of drug candidates to the CYPs. In routine screening protocols, the accurate determination of CYP affinity is often hampered by several factors, including compound or metabolite fluorescence in a fluorescent substrate assay, limited compound solubility, and atypical kinetics.[3]

Atypical or non-Michaelis−Menten kinetics is most likely a result of multiple substrates or effectors simultaneously binding to the CYP. The result is nonhyperbolic saturation kinetics for a single substrate or mixed inhibition kinetics or activation for two substrates.[3] Interpretation of atypical kinetics can be complicated. The impact of one molecule on the metabolism of another can vary with different substrates. A molecule may inhibit the metabolism of one substrate and activate the metabolism of another. This suggests that inhibition of a single probe substrate may not adequately predict the drug interaction potential of that compound for all drugs.

Although atypical kinetics are most commonly observed for CYP3A4,[3−6] they have been reported for other enzymes including CYP2C9,[5,7−9] CYP2D6,[10,11] and CYP1A2.[12] However, the frequency of atypical kinetics for the different P450 isoforms is generally unknown.

Here we report the generation and analysis of inhibition data over a diverse set of 500 drug-like molecules against recombinant CYP 2C9 and 2D6 enzymes. A method to distinguish typical from atypical kinetics is presented. By measuring a diverse compound set, we have obtained statistics on the frequency of limited solubility, fluorescence interference, and atypical kinetics for 2C9 and 2D6. In addition to these statistics, the dataset we have collected provides a diverse data set free of compounds with uncertain affinity due to atypical kinetics, which can be used for the construction of quantitative structure−activity relationship (QSAR) models.

Methods

Compound Selection. A set of 500 compounds were selected from the Merck sample repository based on two different criteria. First, some well-known generic drugs for which a sample was present in the Merck repository were retrieved, excluding compounds with low purity as determined by mass spectrometry or for which insufficient sample was available. Second, an additional

---

* To whom correspondence should be addressed. Tel.: (732) 594-6812. Fax: (732) 594-4224. E-mail: daniel_mcmasters@merck.com.
† Department of Molecular Systems.
‡ Visiting scientist from Washington State University, Pullman, Washington.
§ Department of Drug Metabolism.
∥ Department of Applied Computer Science and Mathematics.
a Abbreviations: AIC, Akaike Information Criterion; AICc, corrected Akaike Information Criterion; DDI, drug−drug interactions; ESI, enzyme−substrate−inhibitor; QSAR, quantitative structure−activity relationship; RSS, residual sum of squares.

diverse set of Merck proprietary compounds was added, making sure that (1) the same availability and purity criteria applied, (2) they were drug-like in the sense of Lipinski's rule-of-five,[13] and (3) none of them had high structural similarity to any of the generic drugs.

Enzymology. To characterize the inhibition (or activation) kinetics of a cytochrome P450 reaction, both single and multiple binding site equations must be used.[14] Competitive inhibition occurs when the binding of one compound to the active site prevents the binding of other substrates, and saturating concentrations of a competitive inhibitor eliminates substrate metabolism. For competitive inhibition, one should use standard hyperbolic inhibition equations that are consistent with 100% activity remaining at zero inhibitor concentration and approach 0% activity remaining at very high inhibitor concentration. Atypical kinetics occurs when one compound does not completely displace the second substrate at saturating concentrations. This can result in partial inhibition, activation, or more complex behavior such as activation followed by inhibition. For partial inhibition, increasing the concentration of inhibitor decreases the rate of substrate metabolism until a plateau is reached, corresponding to the rate of metabolism observed for the enzyme−substrate−inhibitor (ESI) complex. For activation, an increase in the rate of metabolism is observed until a plateau is reached, corresponding to the increased rate of metabolism observed for the ESI complex. When two substrates can simultaneously bind to the enzyme, more complex behavior is also possible. The most easily observed behavior is activation followed by inhibition. This presumably occurs when binding of a test compound results in an increase in substrate metabolism. However, at higher concentrations of the test compound, the substrate can be displaced from the active site by a second molecule of the test compound. The result is activation at low concentrations of test compound followed by inhibition at higher concentrations.

P450 Inhibition Assay. All reagents were purchased from Sigma-Aldrich (St. Louis, MO), except AMMC, which was purchased from BD Gentest (Franklin Lakes, NJ). The inhibition versus concentration data for each compound was determined in cDNA expressed CYP2C9 and CYP2D6 microsomes in a 96 microtiter plate format. The CYP marker substrate was 3-[2-(N,N-diethylamino)ethyl]-7-methoxy-4-methylcoumarin (AMMC) for CYP2D6 and 7-methoxy-4-(trifluoromethyl)coumarin (MFC) for CYP2C9. Inhibition was measured by the addition of the test compound dissolved in 50:50 acetonitrile/water to an assay solution containing deionized water, 0.5 M KPO_4, pH 7.4, glucose-6-phosphate dehydrogenase (1000 units per mL), and a cofactor solution consisting of B-NADP (20 mg/mL), $MgCl_2$ (13.3 mg/mL), and glucose-6-phosphate (20 mg/mL). The final inhibitor solvent concentration in the assay was 1%. The plate was then preread on a Tecan Safire fluorescent plate reader (Tecan, Männedorf, Switzerland) under the following conditions: for CYP2C9, ex. 430 nm, em. 535 nm, 12 nm bandwidth, gain = 75, 20 μs integration time, 20 flashes; for CYP2D6, ex. 390 nm, em. 465 nm, 12 nm bandwidth, 20 μs integration time, 20 flashes.

A solution prepared from cDNA expressed microsomes (final enzyme concentrations of 25 pmol/mL for CYP2C9 and 20 pmol/mL for CYP2D6) plus substrate (final concentration of 50 μM MFC for CYP2C9 and 1.5 μM AMMC for CYP2D6, equal to the K_m in both cases) was then added to the serially diluted test compound. After incubation (15 min for CYP2C9 and 45 min for CYP2D6) at 37 °C, the reaction was stopped by the addition of a 0.5 M Tris/acetonitrile solution. The plate was then read on a Tecan Safire fluorescent plate reader under the same conditions as described above. The incubations did not contain cytochrome b5; Hummel et al. have shown that the presence of cytochrome b5 can alter a compound's CYP2C9 inhibition profile.[15]

Fluorescence Interference. Several controls on the assay plate were used to determine fluorescence interference from components in the assay mixture. These included a control to assess the contribution of fluorescence of enzyme and cofactors, a control to assess the contribution of fluorescence from the substrate, a control to assess any quenching effects on product response from any meta-bolite formed, and controls to assess the contribution of fluorescence from potential inhibitors and from the metabolites formed.

Solubility Determination. Stock compound was diluted in a solution of 0.5 M KPO_4, pH 7.4, and deionized water to mimic the initial compound dilution in the fluorescent inhibition assay. These compound dilutions and the stock compound solution in 50% acetonitrile/water were injected through the BD Biosciences Solubility Scanner (Franklin Lakes, NJ), which measures particle sizes from 100 nm to 5 microns using 90° light scatter in a flow cell using a 635 nm laser. Particle counts from the stock compounds and the diluted compounds were compared to background values of the solution of 0.5 M KPO_4, pH 7.4. Compounds exhibiting greater than 2000 particle counts were excluded from further analysis.

Data Analysis. Titration curves were analyzed by fitting the percent control versus compound concentration data to four separate equations, corresponding to a simple mean and one-, two-, and three-parameter hyperbolic fit functions. The nonlinear fits were performed using Mathematica, version 5.2 (Wolfram Research, Inc., Champaign, IL, 2005). For each fit, the residual sum of squares (RSS) and fit parameters were derived and used to interpret the fits, as described below.

The first function, shown in eq 1, determines the mean of the data points and is intended to fit titration curves of compounds with no affinity for the enzyme. The second equation is a one-parameter hyperbolic function, which fits competitive kinetics; the parameter c_2 indicates the binding affinity, which under ideal Michaelis−Menten kinetics equals the IC_{50}. Equation 3 is a two-parameter hyperbolic fit; the parameter c_3 is analogous to parameter c_2 in eq 2, while parameter b_3 indicates the final inhibition. A value of b_3 between 0 and 1 would, therefore, indicate apparent partial inhibition, while a negative value of b_3 indicates apparent activation. Finally, a three-parameter equation (eq 4) was introduced to handle more complex behavior, such as activation at a low concentration followed by inhibition at a higher concentration.

$$y = a_1 \tag{1}$$

$$y = 100\left(1 - \frac{x}{x + c_2}\right) \tag{2}$$
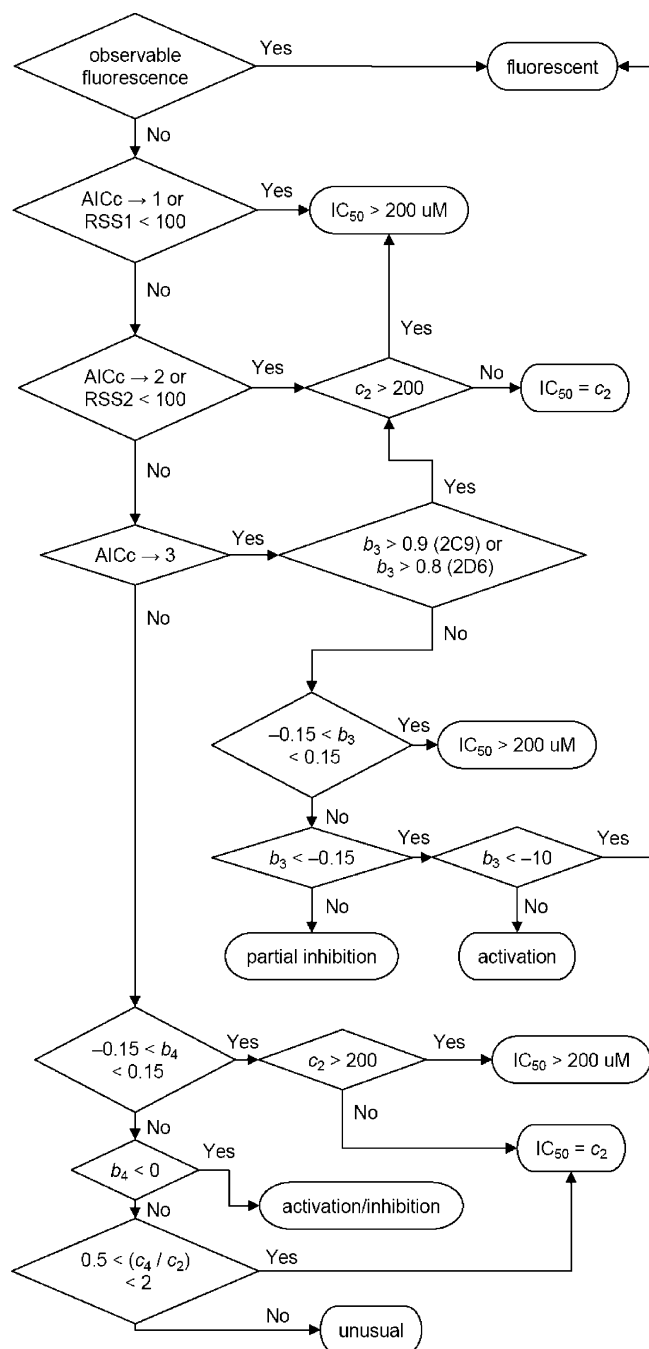
$$y = 100\left(1 - \frac{b_3 x}{x + c_3}\right) \tag{3}$$

$$y = 100\left(1 - \frac{b_4 x + \left(\frac{x_2}{d_4}\right)}{x + c_4 + \left(\frac{x_2}{d_4}\right)}\right) \tag{4}$$

Initial guesses for the parameters were as follows: $c_2 = 10$, $b_3 = -2$, $c_3 = 1$, $b_4 = -2$, $c_4 = 10$, and $d_4 = 10$. To determine which fit best described the data, we utilized the Akaike Information Criterion (AIC) equation, corrected for small datasets (AICc, eq 5).[16]

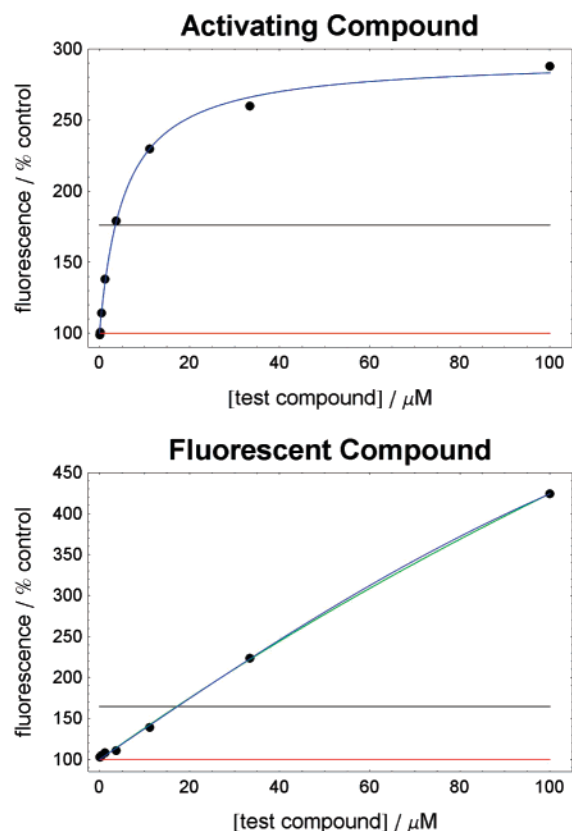$$\text{AICc} = 2k + n \ln\left(\frac{\text{RSS}}{n}\right) + \frac{2k(k + 1)}{n - k - 1} \tag{5}$$

RSS is the residual sum of squares from the fit, k is the number of parameters, and n is the number of datapoints. A lower value of AICc is obtained for better fits (smaller RSS) and for simpler models (smaller k); therefore, AICc is a formal method to evaluate model quality and simplicity. Because of the presence of some experimental uncertainty in the determination of percent control at each concentration, occasionally a very good fit could be obtained with one of the simple equations, but addition of more parameters caused an even better fit to the experimental noise; therefore, further criteria were introduced based on the fit parameters. Compounds that exhibited fluorescence or poor solubility, as determined by the

Figure 1. Flowchart describing data analysis based on AICc and fit parameters.

Figure 2. Dose−response curves for a compound displaying activation (top, $b_3 = -1.932$, $c_3 = 5.44 \ \mu M$) and one displaying fluorescence (bottom, $b_3 = -19.130$, $c_3 = 489.6 \ \mu M$). Concentration of test compound is on the x-axis and percent control fluorescence is on the y-axis. Individual data points appear as filled circles. Fits to eqs 1−4 appear in black, red, green, and blue, respectively.

particle count, were excluded from further analysis. A flowchart for assignment of the titration curves is presented in Figure 1.

Compounds were deemed inactive if eq 1 yielded the smallest AICc, if the RSS for eq 1 was less than 100 or if eq 2 yielded the smallest AICc, but c_2 was >200 μM. Compounds for which eq 2 yielded the smallest AICc, or for which RSS2 was <100, and with c_2 <200 μM were deemed competitive inhibitors. For curves that fit to eq 3, the interpretation depends on the value of b_3. For very small values of b_3, between −0.15 and 0.15, the curve could not reliably distinguish a flat line from a compound showing very slight partial inhibition or activation due to the level of noise in the assay; these were, therefore, considered inactive. Values of $b_3 < -0.15$ indicate possible activation. However, fluorescence is another possible cause of apparent activation. In the case of fluorescence, however, the apparent degree of activation should be linear with compound concentration, yielding a straight line and very large values for b_3 and c_3 that have no meaningful physical interpretation.

For example, in our dataset, we found several compounds with a value of b_3 less than -10^{11}, and c_3 greater than $10^{14} \ \mu M$. Of the remaining cases of apparent activation, several compounds with observable fluorescence gave b_3 in the range of −10 to −20, while the largest negative value for b_3 in our set for a compound with no observed fluorescence was −6.3. Based on this distribution and on the degree of activation typically described for CYP activators described in the literature, which ranges up to around 6-fold,[4,5,17−20] we set a minimum cutoff for b_3 at −10. Figure 2 displays activation curves for a compound with true activation and a compound thought to be fluorescent or generating a fluorescent metabolite.

Among compounds where eq 4, the three-parameter fit that allows for more complex kinetics, gave the smallest AICc, many had very small values of b_4 and c_4, which allowed the curve to better fit the data at low concentration due to small shifts in the baseline. Therefore, if b_4 was between −0.15 and 0.15, the data was considered to be a case of normal kinetics. When b_4 was less than −0.15, the percent control activity was observed to increase as seen in activation and then decrease again at higher concentration. These curves were therefore labeled "activation/inhibition". Finally, when $b_4 > 0.15$, the curve showed close to normal kinetics but did not quite fit a hyperbolic curve. In these cases, when the affinity parameter c_4 was within 2-fold of the hyperbolic affinity constant c_2, the deviation from typical kinetics was considered not to be significant and the typical kinetics binding affinity c_2 was used. When c_2 and c_4 differed by more than 2-fold, the observed kinetics were judged "unusual".

Compounds were tested at concentrations up to 100 μM. Although this limits the ability to assign accurate affinity values to around 50 μM or below, for QSAR modeling purposes we wished to have as broad a dynamic range in our data as possible, even at the expense of some slight uncertainty in the exact affinity for weak inhibitors. For our purposes, we used a cutoff for estimating affinity
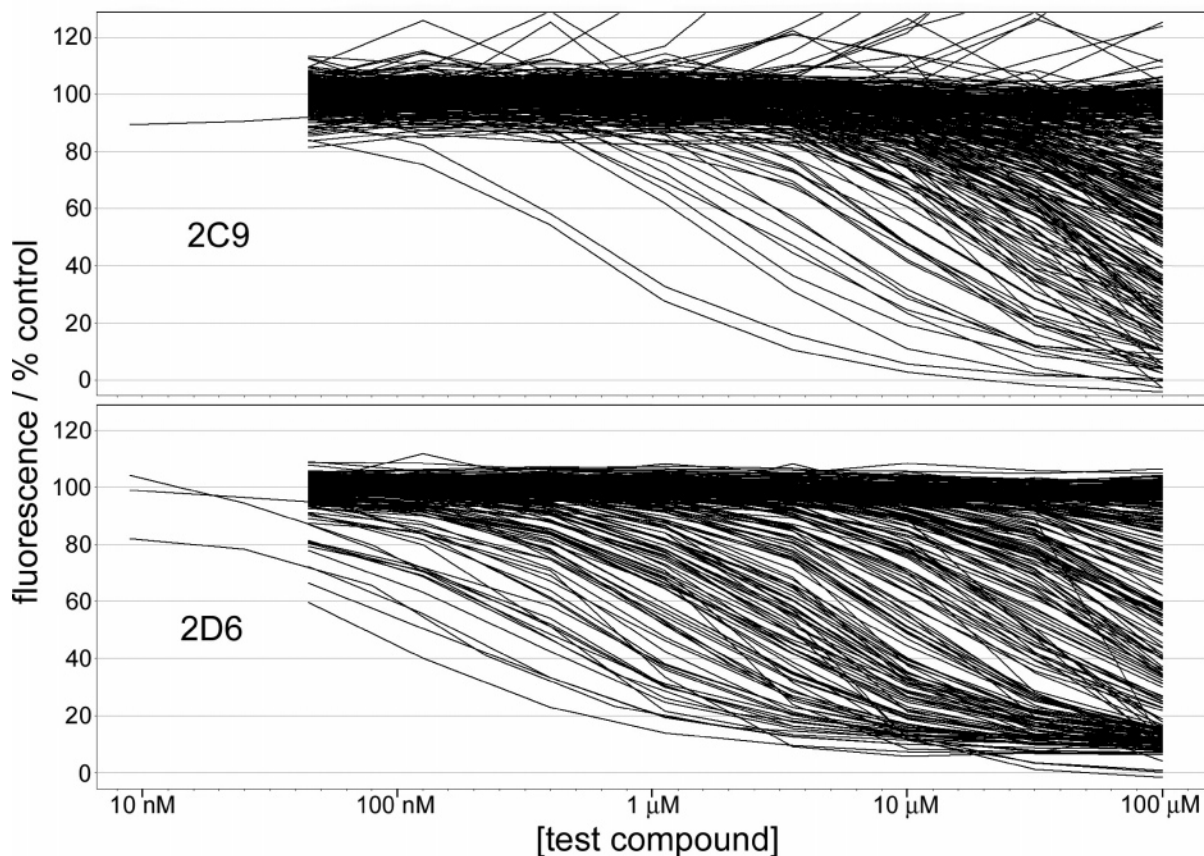
Figure 3. Overlaid inhibition curves for 2C9 (top) and 2D6 (bottom).

Table 1. Frequency of Typical and Atypical Kinetics, Fluorescence, and Solubility Issues for 2C9 and 2D6[a]

classification	number (%) of compounds for 2C9	number (%) of compounds for 2D6
inactive (IC$_{50}$ > 200 μM)	160 (52.8)	159 (51.3)
active	143 (47.2)	151 (48.7)
MM kinetics	117 (38.6)	149 (48.1)
non-MM kinetics	26 (8.6)	2 (0.6)
partial inhibition	7 (2.3)	1 (0.3)
activation	8 (2.6)	0 (0.0)
activation/inhibition	9 (3.0)	1 (0.3)
unusual	2 (0.7)	0 (0.0)
determined	303 (67.3)	310 (67.7)
fluorescence interference	78 (17.3)	69 (15.1)
poor solubility	104 (23.1)	110 (24.0)
solubility not determined	1 (0.2)	3 (0.7)

[a] The number of compounds is listed along with percentages in parentheses.

of 200 μM; compounds with calculated affinity greater than this value were considered inactive.

Calculated Properties. Percent polar surface area was calculated from 3D structures using the method of Clark.[21] Calculated logD values were obtained using ACDLabs logD prediction software, version 8.07 (Advanced Chemistry Development, Inc., Toronto, Ontario, 2004).

Results

Statistics on the number of compounds exhibiting inhibition, partial inhibition, activation, unusual kinetics, or no effect are tabulated in Table 1 for each of the two isoforms. The two isoforms have similar proportions of active and inactive compounds. However, the range of inhibitor potencies observed for the two isoforms differs somewhat. Figure 3 shows the range of inhibition curves for 2D6 and 2C9. For 2C9, a range in

affinities of roughly 2 orders of magnitude could be determined, while for 2D6, the range is around 2.5 orders of magnitude.

Examination of the final value of b_3 over the full set of compounds revealed that a large number of compounds had b_3 in the range of 0.8 to 0.9 for 2D6 but not for 2C9. In Figure 4, the distribution of b_3 for each isoform is plotted as histograms depicting the value of parameter b_3 on the x-axis versus the number of compounds on the y-axis. Plotting each of the isoforms separately reveals a relatively uniform distribution of b_3 for 2C9, whereas the 2D6 distribution shows few compounds from 0.1 to 0.8, with a large number of compounds from 0.8 to 1.0, indicating that few compounds decreased the percent control fluorescence completely. We presume that a true partial inhibitor caused by two molecules in the active site would have a relatively random distribution of degree of partial inhibition (indicated by b_3) and that the nonuniform distribution of 2D6 indicates that the large number of compounds with b_3 in the range of 0.8−0.9 do not show partial inhibition but rather normal competitive inhibition. The reason for the small degree of residual fluorescence is unknown.

Table 2 summarizes the findings for the compounds displaying atypical kinetics in our dataset, with the exception of a small number of Merck proprietary structures.

To study the influence of molecular charge and hydrophobicity on compounds' affinities for CYP2C9 and CYP2D6, net molecular charge and percent polar surface area were calculated. Figure 5 shows the average inhibition constant on a logarithmic scale as a function of percent polar surface area and molecular charge, while Figure 6 displays the inhibition of the individual compounds. For this purpose, compounds that were determined to have an inhibition constant greater than 200 μM were assigned a value of 200 μM, and compounds displaying atypical kinetics were excluded.
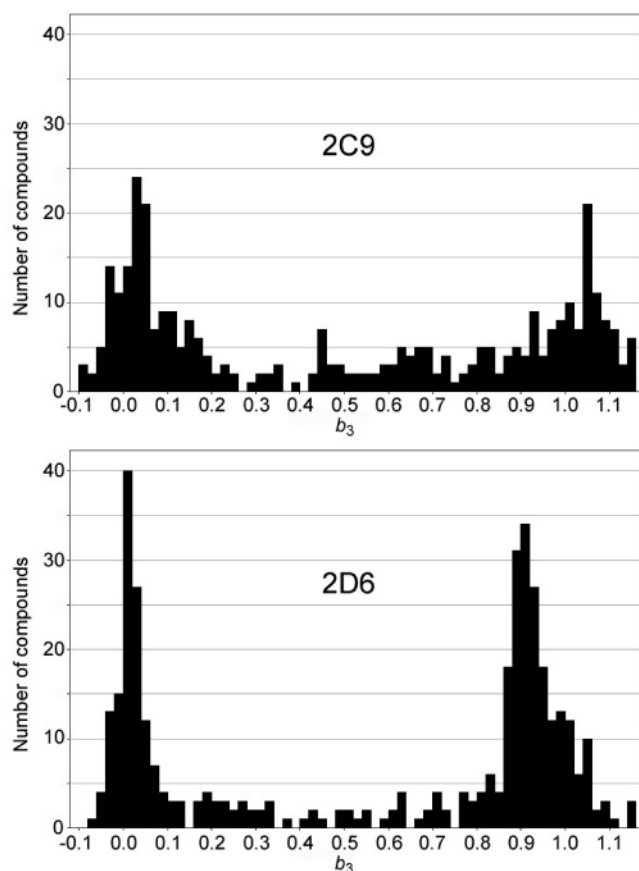
Figure 4. Histograms of the distribution of b_3 for 2C9 (top) compared with 2D6 (bottom).

The distributions of active to inactive compounds and of atypical to competitive inhibitors for 2C9 were also determined as a function of compound class and molecular properties (Table 3). First, although approximately half of the compounds were active, <10% of the compounds with calculated logP values <0.5 were active. Next, for compounds with a carboxylic acid group, a clear separation can be found between logP and polar surface area. Eighteen out of 19 compounds that have logP < 1.0 or PSA > 80 Å^2 are inactive, while 17 out of 20 compounds with logP > 1.0 and PSA < 80 Å^2 are active. Of those active carboxylic acids, 8 out of 17 display atypical kinetics. This percentage (47%) is much higher than the 18% that is observed for all active compounds. Like carboxylic acids, the activity of sulfonamides depended on compound hydrophobicity; however, only 2 of the 25 active sulfonamides showed atypical kinetics. For the compounds with a basic nitrogen and a logP < 1.0, 25 of 26 are inactive. Finally, 10 out of 10 quaternary amines are inactive for CYP2C9.

Discussion

Inhibition of cytochrome P450 enzymes by drugs is a major cause of DDI and is, therefore, closely monitored during the drug discovery process. Although thousands of compounds are measured for their ability to inhibit the major drug-metabolizing isoforms 3A4, 2D6, 2C9, and 1A2, the actual affinity of the drug molecule to the enzyme may often be poorly determined due to insolubility, fluorescence, or atypical kinetics.

Solubility. Solubility has become more of an issue in analytical assays because the hydrophobicity of drug candidates is increasing.[22] Precipitation of a compound during an analytical procedure can result in false values. For P450 inhibition experiments, the expected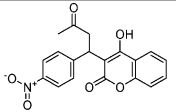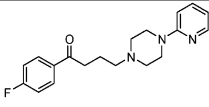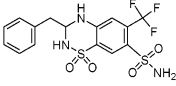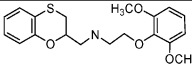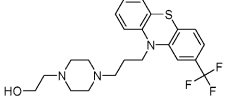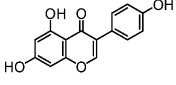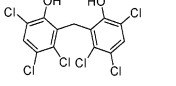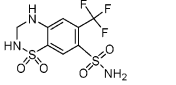 substrate concentrations cannot be increased beyond their solubility limit. The resulting inhibition curves have the appearance of partial inhibition when the solubility limit is reached before the enzyme is saturated. When standard amounts of liver microsomes are used for inhibition experiments, for example, 250 μg microsomal protein, the excess lipid can increase the apparent solubility of the test compound. In reality, the solubility of the test compound is the same and the concentration of the free test compound is decreased. The decreased free concentrations in the incubation result in an apparent increase in the IC$_{50}$.[23−26]
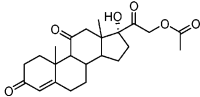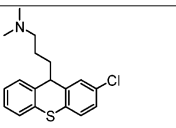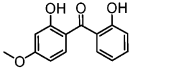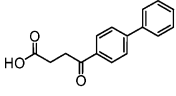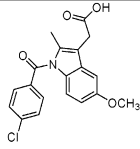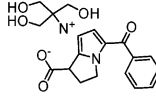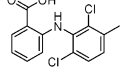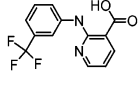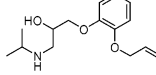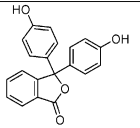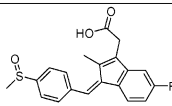
For the experiments reported here, expressed enzymes were used. The higher specific content results in a very small amount of lipids in the incubation, thereby minimizing the partitioning of substrate in the incubation and minimizing the uncertainty in substrate concentration. For the compounds tested, approximately 20% of the compounds were found to have poor solubility. For the purposes of our analysis, we cannot distinguish a compound reaching its solubility limit from the compound having partial inhibition, so these compounds were excluded from further analysis. In a drug discovery environment, however, the apparent partial inhibition by poorly soluble compounds can be evaluated to help determine the potential for clinical interactions.

Fluorescence Interference. When a fluorescent assay is used to measure P450 inhibition, a substrate is used that produces a fluorescent metabolite. The advantage of this assay is speed and accuracy; the disadvantage is that fluorescence from the test compound or its metabolite can interfere with detection of probe metabolite fluorescence. Therefore, it is necessary to run controls with test compound only, both in the presence and absence of NADPH. For this test set, approximately 15% of the compounds failed due to fluorescence interference and were removed.

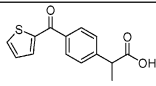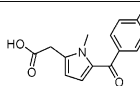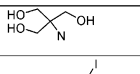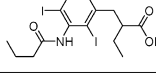**Aggregation.** Figure 3 reveals that, although the vast majority of compounds examined for 2D6 inhibition gave curves with a slope expected for competitive kinetics, with a change from 10% to 90% inhibition over an 81-fold change in concentration, there are several compounds with markedly steeper dose−response curves. Shoichet has recently analyzed steep dose−response curves in inhibition assays and concluded that a common cause of such behavior is compound aggregation.[27] Shoichet and co-workers have examined a number of drugs and drug-like molecules for their propensity to aggregate;[28,29] we therefore looked to see whether any of the compounds in our dataset were among the Shoichet aggregation data or were structurally similar. We found five molecules that overlapped these two sets, namely, clotrimazole, econazole, miconazole, nicardipine, and sulconazole. All five of these compounds were found to have poor solubility in our turbidimetric assay and had, therefore, been removed. The compounds with steep dose−response curves in Figure 3 were not assayed in the Shoichet sets. In most cases, no similar compounds were found in Shoichet set either. One of the steep curves was that of phenolphthalein, which was assigned by our algorithm as exhibiting atypical kinetics for 2D6. Tetraiodophenolphthalein has been reported by Shoichet et al. to form aggregates, and it is possible that phenolphthalein itself has similar behavior. However, the phenolphthalein inhibition curve for 2C9 did not display a steep slope and could be fit well with a hyperbolic equation. It is conceivable that compounds may show aggregation with particles too small to be detected by the turbidimetric assay performed by us, but the observation that all the known aggregators were identified by turbidimetry suggests that this is unlikely to explain most of the steep curves we observed. It should also be noted that

Table 2. Structures and Kinetic Parameters for Compounds Displaying Atypical Kinetics

| Compound	Structure	Observed kinetics	Isoform	b_3	c_3 / µM
Acenocoumarol		Activation	2C9	−1.93	5.4
Azaperone		Activation / inhibition	2C9		
Bendroflumethia-zide		Activation / inhibition	2C9		
Benoxathian		Activation / inhibition	2C9		
Cortisone acetate		Partial inhibition	2C9	0.17	16.2
Dihydro-chlorprothixene		Unusual	2C9		
Dioxybenzone		Activation / inhibition	2C9		
Fenbufen		Activation	2C9	−1.27	423.1
Fluphenazine		Unusual	2C9		
Genistein		Activation / inhibition	2C9		
Hexachlorophene		Activation	2C9	−0.58	7.0
Hydroflumethia-zide		Activation	2C9	−6.31	145.4
Indomethacin		Partial inhibition	2C9	0.73	13.8
Ketorolac tromethamine		Activation	2C9	−3.56	162.1
Meclofenamate		Activation / inhibition	2C9		
Niflumic acid		Partial inhibition	2C9	0.82	21.3
Oxprenolol		Partial inhibition	2C9	0.64	28.7
Phenolphthalein		Activation / inhibition	2D6		
Sulindac		Activation	2C9	−2.14	257.0
Suprofen		Partial inhibition	2C9	0.50	11.8
Tolmetin		Activation	2C9	−1.12	40.3
Tromethamine		Activation / inhibition	2C9		
Tyropanoate		Activation	2C9	−0.69	27.5

the 3-fold dilution series we performed may not provide sufficient data to reliably identify steep dose−response curves, as the change of a single data point due to experimental error could result in an apparently steep slope.

Frequency of Non-Michaelis−Menten Kinetics for 2C9 and 2D6. Removal of compounds whose analyses are complicated by solubility or fluorescence allows the frequency of non-Michaelis−Menten kinetics to be more reliably determined. In order to objectively evaluate the dataset, the rule-based method described under Methods and outlined in Figure 1 was created. As seen in Table 1, the occurrence of non-Michaelis−Menten kinetics is much higher for 2C9 than for 2D6. Only two cases of non-Michaelis−Menten kinetics were observed for isoform 2D6. In contrast, the rate of atypical kinetics for 2C9 was approximately 9% of all compounds and 18% of all actives, with a roughly equal number of cases of partial inhibition, activation, and activation followed by inhibi-

tion at higher concentration. These data are similar to results observed previously when CYP2C9 and CYP2D6 reactions were characterized using 26-point K_i determinations and mass spectrometric analyses (Camitro Corporation, unpublished results).

It should be noted that we may have missed a few CYP2C9 compounds that bind to the active site but show no apparent activation or inhibition. Compounds that showed less than 10% activation or partial inhibition could still be binding to the active site yet be classified as inactive. The same could be said for CYP2D6, but the almost complete absence of non-Michaelis−Menten kinetics for this enzyme makes it unlikely.

Interpretation of Non-Michaelis−Menten Kinetics. When non-Michaelis−Menten kinetics is observed in an inhibition assay, caution must be taken in interpreting the results. For P450 reactions, partial inhibition or activation suggests that both
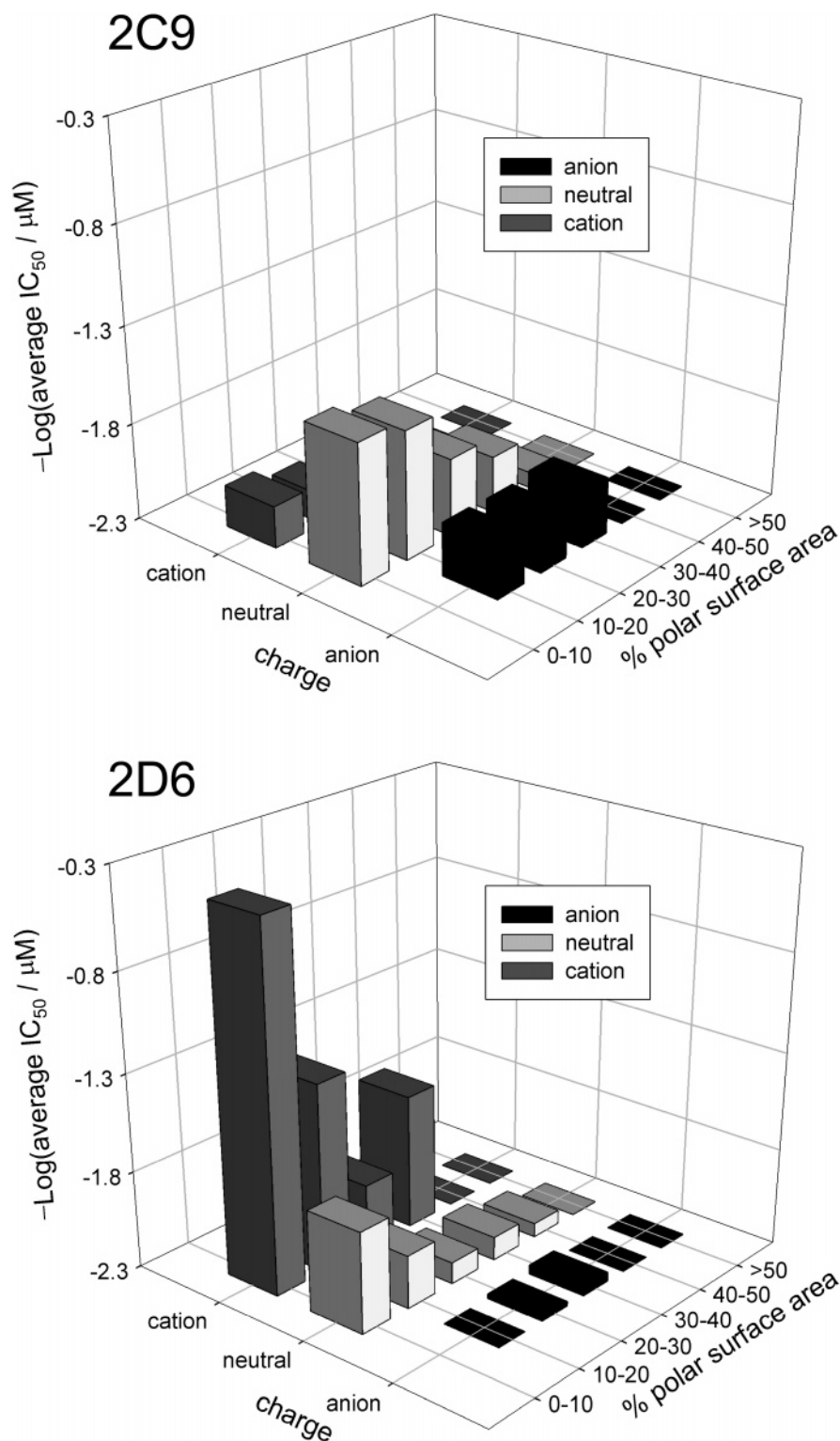
Figure 5. Histogram showing the relationship between molecular charge and percent polar area on inhibition of CYPs 2D6 (left) and 2C9 (right). The average inhibition constant is indicated by bar height and is expressed as $-\log(IC_{50})$.

substrate and test compound are present in the active site. The resulting inhibition or activation curve is a result of affinities and velocities of the enzyme−substrate, enzyme−effector, and enzyme−substrate−effector complexes. As described previously,[5,30,31] the binding constants for these reactions are substrate dependent, that is, change when a different probe substrate is used.

Non-Michaelis−Menten kinetics can have an effect on the prediction of DDI. For a drug primarily eliminated by the P450

pathway being studied, the increase in exposure due to a competitive inhibitor is given by eq 6

$$\frac{AUC_i}{AUC} = 1 + \frac{[I]}{K_i} \qquad (6)$$

where AUC_i/AUC is the increase in exposure due to inhibition, $[I]$ is the inhibitor concentration at the active site, and K_i is the competitive inhibition constant. For competitive inhibition, the
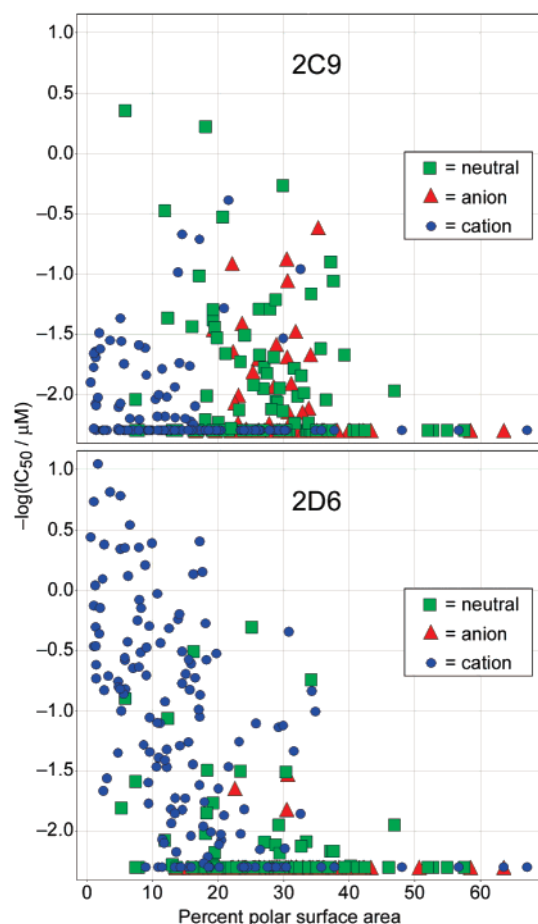
Figure 6. Plot of percent polar surface area versus 2C9 (top) and 2D6 (bottom) inhibition for cations (blue), anions (red), and neutral compounds (green).

Table 3. Categorization of CYP2C9 Compounds by Subclass[a]

cmpd category	category	active/inactive[b,c]	atypical/competitive [c]
all CYP2C9	all	143:159	26:117
all CYP2C9	log P < 0.5	4:47***	2:2
all CYP2C9	log P ≥ 0.5	139:112*	24:115
carboxylic acids	all	18:21	9:9***
carboxylic acids	log P < 1.0 or PSA > 80	1:18***	1:0*
carboxylic acids	log P > 1.0 and PSA < 80	17:3***	8:9**
sulfonamides	log P < 0	0:5*	0:0
sulfonamides	log P > 0	25:6***	2:23
basic nitrogen	log P < 1.0	1:25***	1:0*
basic nitrogen	log P > 1.0	52:58	6:46
quaternary amines		0:10**	0:0

[a] *$p < 0.05$; **$p < 0.01$; ***$p < 0.001$. [b] Active compounds include competitive inhibitors and compounds with atypical kinetics. [c] Significance reported for rows 2−11 is the p-value for the difference from all CYP2C9 results reported in row 1 determined using the chi-squared test.

inhibition constant is not substrate dependent. When non-Michaelis−Menten kinetics are observed, the K_i value from one reaction may not be the same as the K_i value for another. Therefore, it may be necessary to determine the inhibition potential for possible co-administered drugs. Due to the high frequency of non-Michaelis−Menten kinetics for CYP3A4, inhibition constants are usually measured with at least two different substrates.[24]

Structural Characteristics of Competitive and Non-Michaelis−Menten Binders. These results and the results of others suggest that the frequency of non-Michaelis−Menten

kinetics is minimal for CYP2D6, ~20% for CYP2C9, and most common for CYP3A4. The simplest explanation for these differences would be differences in active site size. Although CYP3A4 can certainly metabolize very large substrates such as erythromycin and cyclosporine, there is no clear size difference between CYP2C9 and CYP2D6 substrates. The active site of CYP2D6 is smaller than those of CYP3A4 and CYP2C9 in the apo crystal structures.[32] However, the size of an active site may be substrate dependent. A recent paper reported that the active site volumes for CYP3A4 were 950, 1650, and 2000 Å[3], for ligand-free, ketoconazole-bound, and erythromycin-bound crystal structures, respectively.[33] The active site volumes of CYP2C9 in ligand-free, flurbiprofen-bound, and warfarin-bound crystal structures are similar; however, the shape of the active site cavities differs in these structures due to changes in the loops between helices B and C and between helices F and G.[34,35] Overall, the crystallographic evidence suggests that both the volume and the flexibility of the active site may play a role in the frequency of non-Michaelis−Menten kinetics.

Cytochrome P450 2D6 has previously been found to display a preference for cations, due to the presence of acidic residues Asp216 and Glu301 in the active site, and for hydrophobic compounds.[32,36] These preferences were confirmed in our dataset. As shown in Figure 5, almost all cationic compounds with polar area below 20% were active, while compounds with polar area >40% were nearly all inactive.

For CYP2C9, substrate preference is more complicated. There was much less effect of molecule net charge on activity, with only a slightly higher average activity for neutral compounds relative to anions, while cations were for the most part inactive (Figure 5). The tendency for heteroactivation of this enzyme has been documented in several reports.[5,7−9] In a recent paper, Egnell et al. screened 1504 compounds and found 37 compounds to be heteroactivators of CYP2C9.[7] Although the percentage is lower than the combined activators and activator/inhibitors in this study, characterization as an activator in the Egnell report required at least 50% activation. Of the activators reported by Egnell, six were present in our dataset. Five of those six, amiodarone, flurbiprofen, hydroflumethiazide, meclofenamate, and tolmetin, displayed activation in our hands. Three are classified as activators or activator/inhibitors in Table 2; amiodarone and flurbiprofen were excluded from classification due to high particle count in the solubility assay. One compound found to be an activator by Egnell et al., diflunisal, showed competitive inhibition kinetics in our assay. The reason for this discrepancy is unknown.

Analysis of the CYP2C9 data from this study revealed several relationships between compound activity and structural class and properties (Table 3). Nearly all the hydrophobic molecules containing a carboxylic acid were found to be active, and a significantly higher proportion of these active molecules showed atypical kinetics than for the full set of active compounds. The 2C9 active site contains a basic residue, Arg108, on the opposite side of the active site from the heme, which binds to the carboxylate of flurbiprofen and has been implicated in the binding of other acid-containing compounds such as benzbromarone.[35,37] If the compound is small enough, there could remain space in the active site for binding of the substrate as well, resulting in partial inhibition or activation.

Conclusion

In summary, we have measured the inhibition of CYP2C9 and CYP2D6 by a diverse set of drug-like molecules and present here a method for the analysis of the inhibition data. This data

set gives insight into the frequency of inhibition and non-Michaelis−Menten kinetics that can be expected in drug discovery programs, and into the molecular features associated with inhibition and atypical kinetics and also represents a diverse and consistently generated data set for QSAR modeling efforts.

References

(1) Denisov, I. G.; Makris, T. M.; Sligar, S. G.; Schlichting, I. Structure and chemistry of cytochrome P450. *Chem. Rev.* **2005**, *105*, 2253−2277.

(2) Makris, T. M.; Davydov, R.; Denisov, I. G.; Hoffman, B. M.; Sligar, S. G. Mechanistic enzymology of oxygen activation by the cytochromes P450. *Drug Metab. Rev.* **2002**, *34*, 691−708.

(3) Atkins, W. M. Non-Michaelis−Menten kinetics in cytochrome P450-catalyzed reactions. *Annu. Rev. Pharmacol. Toxicol.* **2005**, *45*, 291−310.

(4) Kenworthy, K. E.; Clarke, S. E.; Andrews, J.; Houston, J. B. Multisite kinetic models for CYP3A4: Simultaneous activation and inhibition of diazepam and testosterone metabolism. *Drug Metab. Dispos.* **2001**, *29*, 1644−1651.

(5) Korzekwa, K. R.; Krishnamachary, N.; Shou, M.; Ogai, A.; Parise, R. A.; Rettie, A. E.; Gonzalez, F. J.; Tracy, T. S. Evaluation of atypical cytochrome P450 kinetics with two-substrate models: Evidence that multiple substrates can simultaneously bind to cytochrome P450 active sites. *Biochemistry* **1998**, *37*, 4137−4147.

(6) Shou, M.; Grogan, J.; Mancewicz, J. A.; Krausz, K. W.; Gonzalez, F. J.; Gelboin, H. V.; Korzekwa, K. R. Activation of Cyp3A4−Evidence for the simultaneous binding of two substrates in A cytochrome-P450 active-site. *Biochemistry* **1994**, *33*, 6450−6455.

(7) Egnell, A. C.; Eriksson, C.; Albertson, N.; Houston, B.; Boyer, S. Generation and evaluation of a CYP2C9 heteroactivation pharmacophore. *J. Pharmacol. Exp. Ther.* **2003**, *307*, 878−887.

(8) Hutzler, J. M.; Hauer, M. J.; Tracy, T. S. Dapsone activation of CYP2C9-mediated metabolism: Evidence for activation of multiple substrates and a two-site model. *Drug Metab. Dispos.* **2001**, *29*, 1029−1034.

(9) Hutzler, J. M.; Wienkers, L. C.; Wahlstrom, J. L.; Carlson, T. J.; Tracy, T. S. Activation of cytochrome P450 2C9-mediated metabolism: Mechanistic evidence in support of kinetic observations. *Arch. Biochem. Biophys.* **2003**, *410*, 16−24.

(10) Afshar, M.; Thormann, W. Capillary electrophoretic investigation of the enantioselective metabolism of propafenone by human cytochrome P-450 SUPERSOMES: Evidence for atypical kinetics by CYP2D6 and CYP3A4. *Electrophoresis* **2006**, *27*, 1526−1536.

(11) Kudo, S.; Odomi, M. Involvement of human cytochrome P450 3A4 in reduced haloperidol oxidation. *Eur. J. Clin. Pharmacol.* **1998**, *54*, 253−259.

(12) Miller, G. P.; Guengerich, F. P. Binding and oxidation of alkyl 4-nitrophenyl ethers by rabbit cytochrome P450 1A2: Evidence for two binding sites. *Biochemistry* **2001**, *40*, 7262−7272.

(13) Lipinski, C. A.; Lombardo, F.; Dominy, B. W.; Feeney, P. J. Experimental and computational approaches to estimate solubility and permeability in drug discovery and development settings. *Adv. Drug Delivery Rev.* **1997**, *23*, 3−25.

(14) Tracy, T. S.; Hummel, M. A. Modeling kinetic data from in vitro drug metabolism enzyme experiments. *Drug Metab. Rev.* **2004**, *36*, 231−242.

(15) Hummel, M. A.; Tracy, T. S.; Hutzler, J. M.; Wahlstrom, J. L.; Zhou, Y.; and Rock, D. A. Influence of fluorescent probe size and cytochrome b5 on drug-drug interactions in CYP2C9. *J. Biomol. Screening* **2006**, *11*, 303−309.

(16) Hurvich, C. M.; Tsai, C. L. Regression and time-series model selection in small samples. *Biometrika* **1989**, *76*, 297−307.

(17) Egnell, A. C.; Houston, B.; Boyer, S. In vivo CYP3A4 heteroactivation is a possible mechanism for the drug interaction between felbamate and carbamazepine. *J. Pharmacol. Exp. Ther.* **2003**, *305*, 1251−1262.

(18) Liu, K. H.; Kim, M. J.; Jung, W. M.; Kang, W.; Cha, I. J.; Shin, J. G. Lansoprazole enantiomer activates human liver microsomal CYP2C9 catalytic activity in a stereospecific and substrate-specific manner. *Drug Metab. Dispos.* **2005**, *33*, 209−213.

(19) Ludwig, E.; Schmid, J.; Beschke, K.; Ebner, T. Activation of human cytochrome P-450 3A4-catalyzed meloxicam 5′-methylhydroxylation by quinidine and hydroquinidine in vitro. *J. Pharmacol. Exp. Ther.* **1999**, *290*, 1−8.

(20) Stresser, D. M.; Blanchard, A. P.; Turner, S. D.; Erve, J. C. L.; Dandeneau, A. A.; Miller, V. P.; Crespi, C. L. Substrate-dependent modulation of CYP3A4 catalytic activity: Analysis of 27 test compounds with four fluorometric substrates. *Drug Metab. Dispos.* **2000**, *28*, 1440−1448.

(21) Clark, D. E. Rapid calculation of polar molecular surface area and its application to the prediction of transport phenomena. 1. Prediction of intestinal absorption. *J. Pharm. Sci.* **1999**, *88*, 807−814.

(22) Lipinski, C. A. Drug-like properties and the causes of poor solubility and poor permeability. *J. Pharmacol. Toxicol. Methods* **2000**, *44*, 235−249.

(23) Margolis, J. M.; Obach, R. S. Impact of nonspecific binding to microsomes and phospholipid on the inhibition of cytochrome P4502D6: Implications for relating in vitro inhibition data to in vivo drug interactions. *Drug Metab. Dispos.* **2003**, *31*, 606−611.

(24) Obach, R. S.; Walsky, R. L.; Venkatakrishnan, K.; Houston, J. B.; Tremaine, L. M. In vitro cytochrome P450 inhibition data and the prediction of drug-drug interactions: Qualitative relationships, quantitative predictions, and the rank-order approach. *Clin. Pharmacol. Ther.* **2005**, *78*, 582−592.

(25) Tran, T. H.; von Moltke, L. L.; Venkatakrishnan, K.; Granda, B. W.; Gibbs, M. A.; Obach, R. S.; Harmatz, J. S.; Greenblatt, D. J. Microsomal protein concentration modifies the apparent inhibitory potency of CYP3A inhibitors. *Drug Metab. Dispos.* **2002**, *30*, 1441−1445.

(26) Venkatakrishnan, K.; von Moltke, L. L.; Obach, R. S.; Greenblatt, D. J. Microsomal binding of amitriptyline: Effect on estimation of enzyme kinetic parameters in vitro. *J. Pharmacol. Exp. Ther.* **2000**, *293*, 343−350.

(27) Shoichet, B. K. Interpreting steep dose−response curves in early inhibitor discovery. *J. Med. Chem.* **2006**, *49*, 7274−7277.

(28) Feng, B. Y.; Shelat, A.; Doman, T. N.; Guy, R. K.; Shoichet, B. K. High-throughput assays for promiscuous inhibitors. *Nat. Chem. Biol.* **2005**, *1*, 146−148.

(29) Seidler, J.; McGovern, S. L.; Doman, T. N.; Shoichet, B. K. Identification and prediction of promiscuous aggregating inhibitors among known drugs. *J. Med. Chem.* **2003**, *46*, 4477−4486.

(30) Galetin, A.; Clarke, S. E.; Houston, J. B. Multisite kinetic analysis of interactions between prototypical CYP3A4 subgroup substrates: Midazolam, testosterone, and nifedipine. *Drug Metab. Dispos.* **2003**, *31*, 1108−1116.

(31) Houston, J. B.; Galetin, A. Modelling atypical CYP3A4 kinetics: Principles and pragmatism. *Arch. Biochem. Biophys.* **2005**, *433*, 351−360.

(32) Rowland, P.; Blaney, F. E.; Smyth, M. G.; Jones, J. J.; Leydon, V. R.; Oxbrow, A. K.; Lewis, C. J.; Tennant, M. G.; Modi, S.; Eggleston, D. S.; Chenery, R. J.; Bridges, A. M. Crystal structure of human cytochrome P450 2D6. *J. Biol. Chem.* **2006**, *281*, 7614−7622.

(33) Ekroos, M.; Sjogren, T. Structural basis for ligand promiscuity in cytochrome P450 3A4. *Proc. Natl. Acad. Sci. U.S.A.* **2006**, *103*, 13682−13687.

(34) Williams, P. A.; Cosme, J.; Ward, A.; Angove, H. C.; Matak Vinkovic, D.; Jhoti, H. Crystal structure of human cytochrome P4502C9 with bound warfarin. *Nature* **2003**, *424*, 464−468.

(35) Wester, M. R.; Yano, J. K.; Schoch, G. A.; Yang, C.; Griffin, K. J.; Stout, C. D.; Johnson, E. F. The structure of human cytochrome P4502C9 complexed with flurbiprofen at 2.0-angstrom resolution. *J. Biol. Chem.* **2004**, *279*, 35630−35637.

(36) Strobl, G. R.; von Kruedener, S.; Stockigt, J.; Guengerich, F. P.; Wolff, T. Development of a pharmacophore for inhibition of human liver cytochrome-P-450 2D6−Molecular modeling and inhibition studies. *J. Med. Chem.* **1993**, *36*, 1136−1145.

(37) Dickmann, L. J.; Locuson, C. W.; Jones, J. P.; Rettie, A. E. Differential roles of Arg97, Asp293, and Arg108 in enzyme stability and substrate specificity of CYP2C9. *Mol. Pharmacol.* **2004**, *65*, 842−850.